Chemical Geology 414 (2015) 16–27

Contents lists available at ScienceDirect

Chemical Geology

journal homepage: www.elsevier.com/locate/chemgeo

Chemical, structural and hyperfine characterization of goethites with simultaneous incorporation of manganese, cobalt and aluminum ions

M. Alvarez [a], A.E. Tufo [b,*], C. Zenobi [a], C.P. Ramos [c], E.E. Sileo [b]

[a] INQUISUR, Departamento de Química, Universidad Nacional del Sur, Avenida Alem 1253, B8000CPB, Bahía Blanca, Argentina
[b] INQUIMAE, Departamento de Química Inorgánica, Analítica y Química Física, Facultad de Ciencias Exactas y Naturales, Universidad de Buenos Aires, Pabellón II, Ciudad Universitaria, C1428EHA, Buenos Aires, Argentina
[c] Gerencia Investigación y Aplicaciones, Centro Atómico Constituyentes — Comisión Nacional de Energía Atómica, Av. Gral. Paz 1499, San Martín (1650), Buenos Aires, Argentina

ARTICLE INFO

Article history:
Received 14 January 2015
Received in revised form 18 August 2015
Accepted 19 August 2015
Available online 28 August 2015

Keywords:
Al-, Co-, Mn-goethites
Multi-substitution
Co-ferrite
Hyperfine properties
Rietveld refinement

ABSTRACT

To elucidate the influence of bi-substitution on the structural and hyperfine properties of goetites, two series of (Al,Co)- and (Mn,Co)-substituted goethites were synthesized in alkaline media by aging several ferrihydrites with different Al/Co and Mn/Co ratios. The samples were fully characterized by chemical analyses, X-ray diffraction (XRD) and Mössbauer spectroscopy; scanning electron microscopy (SEM), zeta potential and BET surface area measurements were also performed. All the solids presented only an α-FeOOH-like structure, with the exception of two preparations with high Co concentrations that developed two phases, goethite and small amounts of the Co-ferrite ($CoFe_2O_4$). The cell parameters in the Co-substituted goethites were markedly smaller than that of the pure sample indicating a oxidation of Co(II) to Co(III) before the incorporation step. In the Co + Mn series the metal substitution followed the trend Co ~ Mn, and in the Co + Al series the trend was Al > Co, and in both cases the incorporation of Co decreased the crystallite size of the samples. The metal-for-Fe incorporation changed the specific surface areas and the morphology of the acicular formed particles. Cobalt containing samples had the highest SSA, while Mn-containing samples had the lowest SSA. The IEP values of the bi-substituted samples were similar to that of pure α-FeOOH, but mono-substitution by Mn and Al diminished the isoelectric points. The low IEP values detected in Mn-goethite (5.8) and Al-goethite (5.2) could be respectively ascribed to an inhomogeneous distribution of Mn(III), and to the different basicity properties of the surface Fe–OH and Al–OH groups. The hyperfine magnetic field B_{hf}, increased quasi linearly with the incorporation of Co in both series. In the Co–Mn series the effect was attributed to variations in particle size distribution, in contrast the marked increase observed in the Co–Al series can be attributed to the decrease in the content of diamagnetic ion Al(III). The results indicate that simultaneous substitutions produce substantial changes in the structural, surface and hyperfine properties of goethites. As the characteristics of the dissolution and adsorption processes of the goethites greatly depend on particle size, BET areas and surface charge of the solids, the reported results will allow us to predict changes in the chemical reactivity and adsorption of the multi-substituted goethites. Also the data on hyperfine properties will help to elucidate the probable substitution in natural samples. The fact that Co-incorporation in bi-substituted samples greatly decreased the particle size increasing the specific surface area is an important parameter for technological applications in adsorption removal processes.

1. Introduction

Goethite (α-FeOOH) is naturally present in various soils, marine sediments and ore deposits. Commonly, natural goethite is not pure, and is associated with a number of cations that are iso- or heterovalent to Fe(III). In fact, in natural environments and in many industrial processes, the oxy-hydroxide forms in the presence of multiple metal cations. Mine effluents contain metals such as Cr, Ni, Zn, Cd, Pb that can be incorporated into α-FeOOH; the same occurs in soils, which may be contaminated with a number of heavy metals from industrial effluents, fertilizers, *etc.* (Vega et al., 2004). Thus the coprecipitation of metals with Fe could lead to the simultaneous incorporation of multiple metals into the goethite structure under natural conditions.

Although single metal-for-Fe substitution has been extensively studied, a few studies have investigated multiple metal substitutions in goethite (Cornell, 1991; Manceau et al., 2000; Alvarez et al., 2007; Kaur et al., 2009a,b; Singh et al., 2010). While Manceau et al. (2000), observed simultaneous incorporation of Cr, Mn, Co, Ni, Cu and Zn in natural goethite, the other authors studied the simultaneous inclusion of cations in the structure of the synthetic goethite. Cornell (1991) reported a maximum incorporation of 8 mol% for Ni, Co and Mn, and Kaur et al. (2009a) reported a maximum value of 10.5 mol% for Cr, Zn, Cd and Pb, into the structure of the oxyhydroxide. The authors also

* Corresponding author.

http://dx.doi.org/10.1016/j.chemgeo.2015.08.022
0009-2541/

reported differences in the maximum level of substitution between single-metal systems and multi-substitution that indicated both synergistic and antagonistic incorporation effects. For instance, in single-metal substitution the sequence for maximum incorporation was Zn ~ Cr > Cd > Pb, and in multiple metal systems the sequence changed to Cr ≥ Cd > Zn > Pb. Regarding the incorporation of aluminum and manganese in goethite, previous research in the authors' laboratory has shown the dominance of Mn over Al in the simultaneous incorporation of both ions in the solid structure (Alvarez et al., 2007).

The substitution of Fe by foreign ions affects the physicochemical properties of the oxy-hydroxide. In particular, cation substitution produces changes around the Fe nucleus that modify the Mössbauer spectrum. For instance, the spectrum of pure well crystallized goethite at room temperature consists of a single sextet with narrow lines, intensity ratios 3:2:1:1:2:3 and a hyperfine magnetic field (B_{hf}) of about 38 T (Cornell and Schwertmann, 2000); however, isomorphous substitutions change the spectrum of α-FeOOH inducing a decrease in the average B_{hf}. The amount of this decrease varies for different incorporated cations (Schwertmann and Taylor, 1989; dos Santos et al., 2001; Krehula and Musić, 2008, 2009; Guimarães et al., 2009), and also depends on the synthesis route of the solid as it modifies the particle and crystallite size of the formed particles. It is well known that changes in crystallinity and particle size generate variations in the hyperfine properties of goethite (Murad and Bowen, 1987; Vandenberghe, 1991; De Grave et al., 2002; Krehula et al., 2005; Krehula and Musić, 2006), inducing the broadening of the resonant lines and modifying the ideal intensity ratios. For example, in the case of very fine particles (<20 nm), the spectrum of goethite collapses to a doublet (Murad and Johnston, 1987), meanwhile increasing particle size and higher crystallinity cause an increase in B_{hf}. Therefore, B_{hf} is particularly sensitive to: particle size distribution, crystallinity and cation substitution that are known to be influenced by Me-for-Fe substitution.

Because the knowledge of the mechanisms by which trace metals associate with goethite in multi-element systems is essential to assess the role played by goethite in the bioavailability of certain ions under natural conditions, in this work we have studied the synthesis of goethite formed from ferrihydrite in the simultaneous presence of three foreign metal cations that are associated with iron oxides in soils and sediments: Al, Co and Mn. Even though the individual effect of each cation on the final products of the crystallization of ferrihydrite have already been fully investigated (Sileo et al., 2001; González et al., 2002; Alvarez et al., 2005, 2008 and references therein), as well as the variations induced by their individual incorporation in the Mössbauer spectrum of goethite (Murad and Bowen, 1987; De Grave et al., 2002; Krehula and Musić, 2006, 2008), the effect of the simultaneous presence of the Co + Mn or Co + Al cations during the formation of goethite, is unknown. For this reason in this study we explore the influence of the simultaneous presence of these cations during the transformation of ferrihydrite to goethite, establishing the maximum uptake of each cation in the presence of the other, and also determining the morphological, structural, surface charge changes, and hyperfine properties in the multi-substituted final goethites. In particular we have used a method sensitive to long-range atomic order (Rietveld refinement) to determine the changes in structure and crystallite size of the oxide, and a method sensitive to short-range atomic order (^{57}Fe Mössbauer spectroscopy) to detect changes in the goethites due to the cations incorporation.

These findings will allow us to fully characterize the substituted goethites and to elucidate the role played by bi-substituted goethites in metal cation sequestration in natural environments, establishing if there are antagonistic or synergetic effects on the sequestration process, while data on hyperfine properties will help in the analyses of natural metal-substituted samples. Additionally, the measurements of the morphology, BET surface areas and surface charge characteristics of the solids will allow us to predict changes in the adsorption and dissolution properties of multi-substituted goethites.

2. Experimental

2.1. Samples preparation

Two series of metal (Me) substituted goethites (Mn,Co-goethites and Co,Al-goethites) were synthesized, keeping a maximum substituting ion concentration (χ_{Me}) at 12 mol mol^{-1}% ($\chi_{Me} = [Me] \times 100/([Me] + [Fe])$). Higher Me concentrations were not used to avoid the formation of additional phases (Alvarez et al., 2007). A sample of pure and a tri-substituted goethite were also prepared.

Series$_I$: Co,Mn-goethites. Samples of Mn-, Co- and mixed Mn,Co-goethites were prepared by a modification of the synthesis proposed by Sileo et al. (2001). Ferrihydrite was precipitated by adding a 2 M NaOH solution to a mixed solution containing $Fe(NO_3)_3$, $Mn(NO_3)_2$ and $Co(NO_3)_2$, until the ratio Me/OH^- was 0.076. For all samples the initial [Fe] + [Mn] + [Co] concentration was 0.53 M. After precipitation, the solids were immediately washed twice with bidistilled water, centrifuged and aged for 15 days at 60 °C in Teflon bottles containing 0.3 M NaOH. Mixed samples were synthesized with different nominal [Co]:[Mn] ratio (9:3, 6:6 and 3:9 mol mol^{-1}), and the solids were named S_I–Co_9Mn_3, S_I–Co_6Mn_6 and S_I–Co_3Mn_9, respectively. Singly substituted Co-goethite and Mn-goethite (samples named S_I–$Co_{12}Mn_0$ and S_I–Co_0Mn_{12}, respectively) were similarly produced by using Fe + Co or Fe + Mn nitrate solutions.

Series$_{II}$: Co,Al-goethites. The samples were prepared following the procedure undertaken by Alvarez et al. (2007). Al-goethite was prepared by mixing two solutions (A and B), where solution A was 25.0 mL of 1 M $Fe(NO_3)_3$, and solution B was 62.5 mL of 0.5 M $Al(NO_3)_3$ + 37.5 mL of 5 M KOH (ratio $OH^-/Al = 6$). Three samples of Co,Al-goethites with different Co:Al ratio (9:3, 6:6 and 3:9 mol mol^{-1}) were obtained by mixing adequate volumes of solutions A and B with 0.5 M $Co(NO_3)_2$, followed by 5 M KOH. The formed suspensions were also aged for 15 days at 60 °C in Teflon bottles, and bi-distilled water was added to reach a final KOH concentration of 0.3 M. Al-goethite (sample named S_{II}–Co_0Al_{12}) was obtained similarly using A and B solutions. The solids were named S_{II}–Co_9Al_3, S_{II}–Co_6Al_6, and S_{II}–Co_3Al_9. Following the same methodology used to synthesize the solids in Series$_{II}$, an additional tri-substituted sample containing Co + Al + Mn was prepared using a 4:4:4 ([Co]:[Al]:[Mn]) ratio (sample $Co_4Al_4Mn_4$).

In all cases the bottles were opened daily, recapped and shaken by hand end-over-end for 5 s. After aging, the materials were washed with bidistilled water until the conductivity of the filtered solution was similar to that of bidistilled water (18 MΩ). The remaining solids were dried at 40 °C and gently crushed in an agate mortar and subsequently treated with 0.4 M HCl at room temperature for 30 min to remove any non-incorporated metal cations or poorly crystalline material from the surface. The metal contents of the samples were determined on these final solids.

2.2. Chemical analysis

The amount of Co, Mn, Al and Fe was measured by atomic absorption spectrometry using a GBC, Model B-932 equipment. The HCl-extracted samples (30 mg) were dissolved at 80 °C in 6 M HCl (Series$_I$) and 12 M HCl (Series$_{II}$).

2.3. X-ray diffraction (XRD) and Rietveld analysis

X-ray diffraction patterns were obtained with a Cu target tube and diffracted beam with a graphite monochromator (Siemens D5000). XRD patterns were measured in the 17.5–130° 2θ range, in 0.025° steps and using 8 s per step counting time. The data were analyzed using the GSAS software package (Larson and Von Dreele, 1996) with EXPGUI interface (Toby, 2002). The mean coherence path dimensions (MCP) or crystallite sizes, were determined in the parallel (P_{paral}) and perpendicular (P_{perp}) directions to the anisotropic broadening (110)

axis. Initial unit-cell parameters and atomic coordinates for goethite were taken from the literature (Szytula et al., 1968), the space group used was Pbnm and the peak profiles were fitted using the Thompson-Cox-Hastings pseudo-Voigt function (Thompson et al., 1987). Crystallite dimensions were calculated making allowances for the instrument broadening function previously modeled for the same instrumental setting using a NIST SRM 660 lanthanum hexaboride (LaB_6) standard.

2.4. Specific surface areas (SSA) and morphological characterization

The surface areas were determined by physical N_2 adsorption/desorption at 77 K, with a Micrometrics ASAP 2020 instrument. Specific surface areas were determined by N_2 adsorption, using a multiple point method.

Particle morphology and size were characterized using scanning electron microscopy (SEM) by examining a drop of suspension dried onto a metallic support (Zeiss Supra 40, field emission, gun-scanning electron microscope).

2.5. Zeta (ζ) potential measurements

The zeta potential or the electrical charge density on the surface (ξ) was obtained using a Malvern Zetasizer. The ξ of the oxides was measured in the range of pH 3.0–9.0. For this, 5×10^{-2} g of the solid was added to 1000 mL, 10^{-2} M $NaNO_3$ solution, using a solution/solid ratio equal to 20 L/g. The pH value was adjusted in the range 3.5 to 8.5 by adding 0.1 M KOH or HNO_3. The electrophoretic cell was rinsed three times with deionized water and with the sample solution before measurements to avoid cross-contamination. The values were expressed as isoelectric point, IEP.

2.6. Mössbauer Spectroscopy

Mössbauer spectra were obtained at room temperature (RT) with a conventional constant acceleration spectrometer in transmission geometry with a ^{57}Co/Rh source. The absorber thickness was optimized according to the Long et al. criterion (Long et al., 1983). Measurements were recorded at 11 mm/s and fitted using the Normos program (Brand, 1991). Isomer shift values were given relative to that of α-Fe at RT.

3. Results and discussion

3.1. Chemical composition and X-ray diffraction (XRD) analysis

The nominal and final content of Mn, Co and Al in the two synthesized series are shown in Table 1. The degree of incorporation of each ion is closely related to the respective initial concentration in solution. The XRD patterns showed goethite as the only crystalline phase in almost all cases. When the goethite was synthesized in the presence of high Co concentrations, as in samples S_{II}–Co_9Al_3 and S_{II}–Co_6Al_6, small amounts of an additional spinel phase were found. As is discussed later, the spinel phase in the samples was ascribed to the presence of Co-ferrite ($CoFe_2O_4$). The calculated phase weight content in S_{II}–Co_9Al_3 was 90.11% (goethite) + 9.89% (Co-ferrite); and 93.50% (goethite) + 8.39% (Co-ferrite) for S_{II}–Co_6Al_6. As all samples were extracted with 0.4 M HCl, these phase weights were not adjusted for any remaining amorphous solids.

The calculated stoichiometry of the substituted goethites taking into account the presence of the spinel phase, is shown in Table 1.

In $Series_I$, as the Mn content increased, the goethites became darker than the pure phase or the Co-goethite. In $Series_{II}$, the color varied from brown sienna to yellow with increasing Al content. The dark color of the S_{II}–Co_9Al_3 and S_{II}–Co_6Al_6 was attributed to the presence of the spinel phase.

3.2. Rietveld refinement results

Lattice parameters and phases composition, as obtained from Rietveld refinement, are presented in Table 2. The refined unit cell volume and cell parameters of S_I–$Co_{12}Mn_0$ (Co-goethite), were markedly smaller than the ones found for pure goethite (136.635(24) *vs.* 138.959(11) Å^3, *a*: 4.5764(4) *vs.* 4.6132(2); *b*: 9.9184(7) *vs.* 9.9599(2) and *c*: 3.0102(7) *vs.* 3.0242(2)). These findings may be attributed to the incorporation of Co as Co(III), indicating oxidation of Co(II) before the incorporation step. The data coincides with the size of the cation ionic radii in a six-coordination site, with values of 0.645 Å for Fe(III), 0.745 Å for Co(II), and 0.61 Å for Co(III) (Shannon, 1976). Further studies based on X-ray Absorption Near Edge Structure (XANES) measurements may be necessary to confirm the oxidation state of the cobalt.

A peak corresponding to a spinel phase was detected in the XRD patterns for S_{II}–Co_9Al_3 and S_{II}–Co_6Al_6 (Fig. 1). The refinement indicated that the cell parameter values for this phase were in the range 8.3842(30) - 8.3957(84) Å. These values coincide with crystallographic data for Co-ferrite (Sileo et al., 2006), and with the Mössbauer analysis discussed

Table 1
Chemical composition of the samples.

Sample	χ_{Mn} (initial)	χ_{Al} (initial)	χ_{Co} (initial)	χ'_{Mn} (incorporated)	χ'_{Al} (incorporated)	χ'_{Co} (incorporated)	Goethite
$Co_0Al_0Mn_0$ (pure goethite)	0.0	0.0	0.0	0.0	0.0	0.0	FeOOH (theoretical stoichiometry)
S_I–$Co_{12}Mn_0$	0.0	–	12.0 ± 0.6	0.0	–	7.4 ± 0.4	$Fe_{0.926}Co_{0.074}OOH$
S_I–Co_9Mn_3	3.0 ± 0.2	–	9.0 ± 0.5	2.1 ± 0.1	–	6.3 ± 0.3	$Fe_{0.916}Co_{0.063}Mn_{0.021}OOH$
S_I–Co_6Mn_6	6.0 ± 0.3	–	6.0 ± 0.3	4.6 ± 0.2	–	4.5 ± 0.2	$Fe_{0.909}Co_{0.045}Mn_{0.046}OOH$
S_I–Co_3Mn_9	9.0 ± 0.5	-	3.0 ± 0.2	7.5 ± 0.4	-	2.3 ± 0.1	$Fe_{0.902}Co_{0.023}Mn_{0.075}OOH$
S_I–Co_0Mn_{12}	12.0 ± 0.6	-	0.0	10.2 ± 0.5	–	0.0	$Fe_{0.898}Mn_{0.102}OOH$
S_{II}–Co_9Al_3	–	3.0 ± 0.2	9.0 ± 0.5	–	2.9 ± 0.1	6.5 ± 0.3	$Fe_{0.922}Co_{0.049}Al_{0.029}$ OOH*
S_{II}–Co_6Al_6	–	6.0 ± 0.3	6.0 ± 0.3	–	4.0 ± 0.2	4.2 ± 0.2	$Fe_{0.927}Co_{0.033}Al_{0.040}OOH$*
S_{II}–Co_3Al_9	–	9.0 ± 0.5	3.0 ± 0.2	–	6.7 ± 0.3	2.2 ± 0.1	$Fe_{0.911}Co_{0.022}Al_{0.067}OOH$
S_{II}–Co_0Al_{12}	–	12.0 ± 0.6	0.0	–	10.5 ± 0.5	0.0	$Fe_{0.895}Al_{0.105}OOH$
$Co_4Al_4Mn_4$	4.0 ± 0.2	4.0 ± 0.2	4.0 ± 0.2	2.8 ± 0.1	3.1 ± 0.2	2.4 ± 0.1	$Fe_{0.917}Mn_{0.028}Co_{0.024}Al_{0.031}OOH$

χ_{Me} expressed as [Me] × 100/([Me] + [Fe]) (mol mol^{-1}%).
Subscripts indicate the nominal content of Mn, Co and Al in each sample.
χ' indicated the total concentration in the final product/or products.
* Stoichiometries estimated from the size of the cell parameters.

Table 2
Unit cell parameters and phase composition obtained by Rietveld refinement.

Sample	$Co_0Al_0Mn_0$	S_I–$Co_{12}Mn_0$	S_I–Co_9Mn_3	S_I–Co_6Mn_6	S_I–Co_3Mn_9	S_I–Co_0Mn_{12}	S_{II}–Co_9Al_3	S_{II}–Co_6Al_6	S_{II}–Co_3Al_9	S_{II}–Co_0Al_{12}	$Co_4Mn_4Al_4$
Phases *(weight fraction)*	Goethite (100%)	Goethite (100%)	Goethite (100%)	Goethite (100%)	Goethite (100%)	Goethite (100%)	Goethite (90.11%) Co-ferrite (9.89%)	Goethite (91.61%) Co-ferrite (8.39%)	Goethite (100%)	Goethite (100%)	Goethite (100%)
a (Å)	4.6132(2)	4.5764(4)	4.5831(4)	4.5895(3)	4.5942(3)	4.5942(2)	4.6081(5)	4.6061(4)	4.6066(3)	4.6030(3)	4.6033(4)
b (Å)	9.9600(2)	9.9184(7)	9.9349(6)	9.9518(5)	9.9714(4)	9.9714(4)	9.9381(6)	9.9277(6)	9.9210(4)	9.9068(4)	9.9365(5
c (Å)	3.0243(2)	3.0102(7)	3.0141(2)	3.0173(1)	3.0178(1)	3.0178(1)	3.0170(2)	3.0144(1)	3.0126(1)	3.0090(1)	3.0162(2)
$a_* = b = c$ (Å)							8.3842(30)	8.3957(84)			
Volume (Å^3)	138.959(11)	136.635(24)	137.244(20)	137.890(17)	138.249(13)	138.248(14)	138.165(24)	137.840(21)	137.688(15)	137.213(14)	137.964(17)
L_{paral} (nm)	68	26	27	30	42	42	46	59	52	63	49
L_{perp} (nm)	95	100	155	318	333	384	227	192	446	564	144
w_{Rp}		14.00	14.34	12.45	15.62	15.57	13.83	13.83	13.07	10.47	15.34
R_p		10.60	11.22	9.98	9.69	10.99	11.06	10.00	10.50	7.96	11.47
Chi^2		1.16	1.254	1.19	1.24	1.23	1.49	1.21	1.18	1.12	1.26
R_{Bragg}		6.94	6.39	5.94	6.11	6.04	7.32	6.42	6.11	6.03	8.38

Notes: $R_p = 100\Sigma||Io - Ic|/\Sigma Io$; $w_{Rp} = 100[\Sigma wi(Io - Ic)^2/\Sigma(wiIo)^2]^{0.5}$; $R_{Bragg} = 100\Sigma||Iko - Ikc|/\Sigma|Iko$; $Chi^2 = \Sigma wi(Io - Ic)^2/(N - P)$. Io and Ic = observed and calculated intensities; wi = weight assigned to each step intensity. Iko and Ikc = observed and calculated intensities for Bragg k-reflection. N and P = number of data points in the pattern and number of parameters refined. Values in parentheses are esd for the least significant figures of the data shown; the esd values are taken from the final cycle of the Rietveld refinement.
* Unit cell parameter for Co-ferrite.

Fig. 1. Partial diffraction patterns of selected samples. All diagrams correspond to a goethite-phase. The presence of a spinel phase (*) is detected in samples S_{II}–Co_9Al_3 and S_{II}–Co_6Al_6. The displacement of the peaks is caused by the different Me-incorporation.

later, indicating that both samples were composed of Co,Al-goethite plus Co-ferrite (respective weight fractions goethite/Co-ferrite are 90.11/9.89 and 91.61/8.39). Calculated final stoichiometric values for the goethite phase in S_{II}–Co_9Al_3 and S_{II}–Co_6Al_6 are $Fe_{0.922}Co_{0.049}Al_{0.029}OOH$ and $Fe_{0.927}Co_{0.033}Al_{0.040}OOH$, respectively. The formation of Co-ferrite indicated that in the preparations with high Co content, part of the Co remained as Co(II) and was incorporated into the spinel, and part was oxidized to Co(III) and incorporated into goethite.

The measured chemical compositions showed that in analogous preparative conditions (*e.g.* samples S_I–Co_6Mn_6 and S_{II}–Co_6Al_6) the incorporation of Mn was similar to that of Co ($\chi'_{Mn} = 4.6 \pm 0.2$ *vs.* $\chi'_{Co} = 4.5 \pm 0.2$), and the incorporation of Al was larger than that of Co ($\chi'_{Al} = 4.0 \pm 0.2$ *vs.* $\chi'_{Co} = 3.3 \pm 0.2$). This contrasts with the results found by Alvarez et al. (2007), who found a clear preference of Mn over Al in the incorporation in goethites, a dominant effect of Co *vs.* Mn was not detected in this work.

In the mono-substituted samples the incorporation followed the trend χ'_{Al} (10.5 ± 0.5) ~ χ'_{Mn} (10.2 ± 0.5) > χ'_{Co} (7.4 ± 0.4). The metal content of the tri-substituted sample indicated that the extent of metal incorporation followed the same trend (χ'_{Al} (3.1 ± 0.2) ~ χ'_{Mn} (2.8 ± 0.1) > χ'_{Co} (2.4 ± 0.1)).

The changes in unit cell dimensions and volume of goethite as a function of the Co-content ($\chi'_{Co\text{-}goe}$) in the phase for Series$_I$ and Series$_{II}$ are displayed in Fig. 2.

In Series$_I$ (Co,Mn), and according to previous works on Mn-substituted goethites (Sileo et al., 2001), the inclusion of Mn(III) in the framework of goethites was evidently expressed in the values of the *b*-parameter of samples with high Mn-content (S_I–Co_3Mn_9 and S_I–Co_0Mn_{12}). In these solids the *b*-value was greater than that of pure goethite, reflecting the influence of the incorporation of Mn(III), a d^4 cation, that imposes a marked Jahn-Teller distortion. Along the series the *a*-parameter decreased with the increase in Co with *a*-values changing from 4.5942(2) Å (in Mn-goethite) to 4.5764(4) Å for the sample with the highest Co-content (S_I–$Co_{12}Mn_0$). Similarly, the *b*- and *c*-parameters diminished with the increase of $\chi'_{Co\text{-}goe}$, with *b*-values varying from 9.9714(4) to 9.9184(7) Å, and *c*-values changing from 3.0178(1) to 3.0102(7) Å. This decrease in cell parameters and consequently cell volume is in agreement with the cell values found in single Co-substituted goethite (Alvarez et al., 2008).

In Series$_{II}$ (Co,Al) all unit cell parameters and cell volume of the Co,Al-goethites increased with an increase of $\chi'_{Co\text{-}goe}$ (and a concomitant decrease in Al-content). Initial and final dimensions for *a*-, *b*-, *c*- and volume values were 4.6030(3)–4.6081(5), 9.9068(4)–9.9381(4),

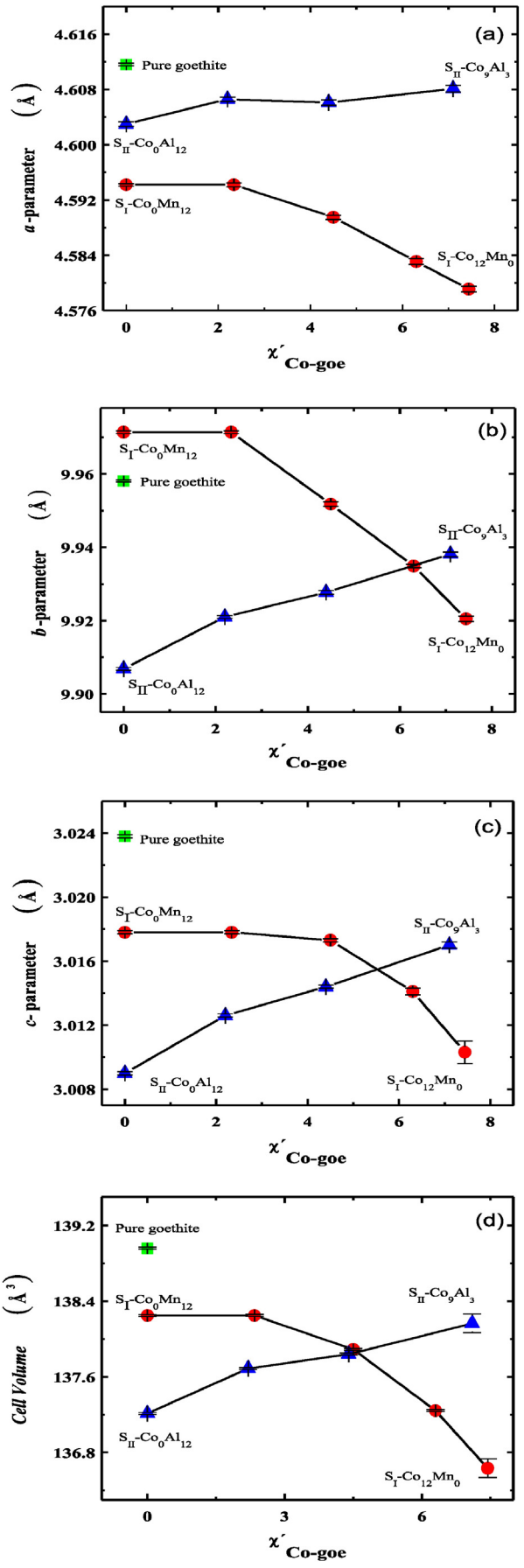

Fig. 2. Variations in unit cell parameters (a–c) and cell volumes (d) in the prepared samples, as a function of Co-incorporation ($\chi'_{Co\text{-}goe}$ mol mol^{-1}) in goethite: (●) $Series_I$ (Co,Mn), (▲) $Series_{II}$ (Co,Al) and (■) pure goethite.

Table 3
Length-to-width ratio, specific surface areas values for both series of samples.

Samples	Width (W) (nm)	Length (L) (nm)	L/W	SSA ($m^2\ g^{-1}$)
$Co_0Mn_0Al_0$	110	903	8.2	36 ± 1
S_I–$Co_{12}Mn_0$	29	567	19.5	109 ± 1
S_I–Co_9Mn_3	39	452	11.6	58 ± 1
S_I–Co_6Mn_6	44	693	15.7	55 ± 1
S_I–Co_3Mn_9	58	827	14.3	42 ± 1
S_I–Co_0Mn_{12}	61	884	13.8	28 ± 1
S_{II}–Co_9Al_3	91	515	5.7	38 ± 1
S_{II}–Co_6Al_6	59	419	7.1	43 ± 1
S_{II}–Co_3Al_9	50	304	6.1	36 ± 1
S_{II}–Co_0Al_{12}	91	386	4.2	26 ± 1
$Co_4Al_4Mn_4$	80	643	8.0	64 ± 1

3.0090(1)–3.0170(2), and 137.213(14)–138.165(24) Å^3, respectively. These findings are in agreement with a series of mixed Mn,Al-goethites prepared in a similar manner by Alvarez et al. (2008), and indicate that the cell-distortion in the Al,Co-substituted goethites is determined primarily by the inclusion of Al, and only samples with low Al-content presented cell parameters close to those of Co-goethite. This is due to the significantly smaller size of the Al(III) ion (ionic radii 0.535 Å, Shannon, 1976) when compared to Co(III) (0.61 Å) and demonstrates that the size of the unit cell is sensitive to the presence of Al, even at low levels of aluminum substitution.

In $Series_I$ the calculated MCP dimensions, reflecting the crystallite size in the parallel (L_{paral}) and perpendicular (L_{perp}) directions to the normal of crystal plane (110) (see Table 2), indicated that Co-incorporation into Mn-goethite diminishes the crystallite size. The L_{paral} and L_{perp} values changed from 42 and 384 nm (in Mn-goethite) to 27 and 155 nm in the Mn,Co-goethite with the highest Co-content (S_I–Co_9Mn_3). In $Series_{II}$, the trend was similar and incorporation of Co to Al-goethite diminished the L_{paral} and L_{perp} values from 63 and 563 nm (in Al-goethite) to 46 and 227 nm (sample S_{II}–Co_9Al_3). The sample containing Fe, Co, Mn and Al, showed one of the lowest crystallinities (49 and 144 nm) even though L_{perp} is higher than for pure goethite. In summary, the incorporation of Co always decreased the mean coherence dimensions or crystallite size.

3.3. Specific surface areas (SSA)

Metal incorporation changed the specific surface areas of the goethites (Table 3). In general, all samples presented a higher surface area than the pure sample; the maximum was found for the mono-substitution of Co-for-Fe that generated particles with a SSA value of 109 ± 1 $m^2\ g^{-1}$. This is consistent with ~~a~~ previous work (Alvarez et al., 2008) reporting that increasing initial Co concentrations and concomitant increases in structural Co incorporation in goethite is positively correlated to increases in specific surface area.

On the contrary, particles containing only Mn had the lowest SSA value (28 ± 1 $m^2\ g^{-1}$). This SSA value was smaller than that of pure goethite and was probably produced by an increase in crystallinity. As can be expected, samples with intermediate di-substitution had increasing SSA values with increasing Co content and a corresponding decrease in Mn content. The SSA values in $Series_I$ followed the trend: S_I–$Co_{12}Mn_0$ > S_I–Co_9Mn_3 > S_I–Co_6Mn_6 > S_I–Co_3Mn_9 > S_I–Co_0Mn_{12} (see Table 3).

In $Series_{II}$, Al-substituted goethite displayed a SSA value of 26 ± 1 $m^2\ g^{-1}$, and the specific surface area increased with increasing Co substitution (and the corresponding diminution in the Al content). However, it must be taken into account that samples S_{II}–Co_6Al_6 and S_{II}–Co_9Al_3 contained small amounts of a powdered spinel phase that influenced

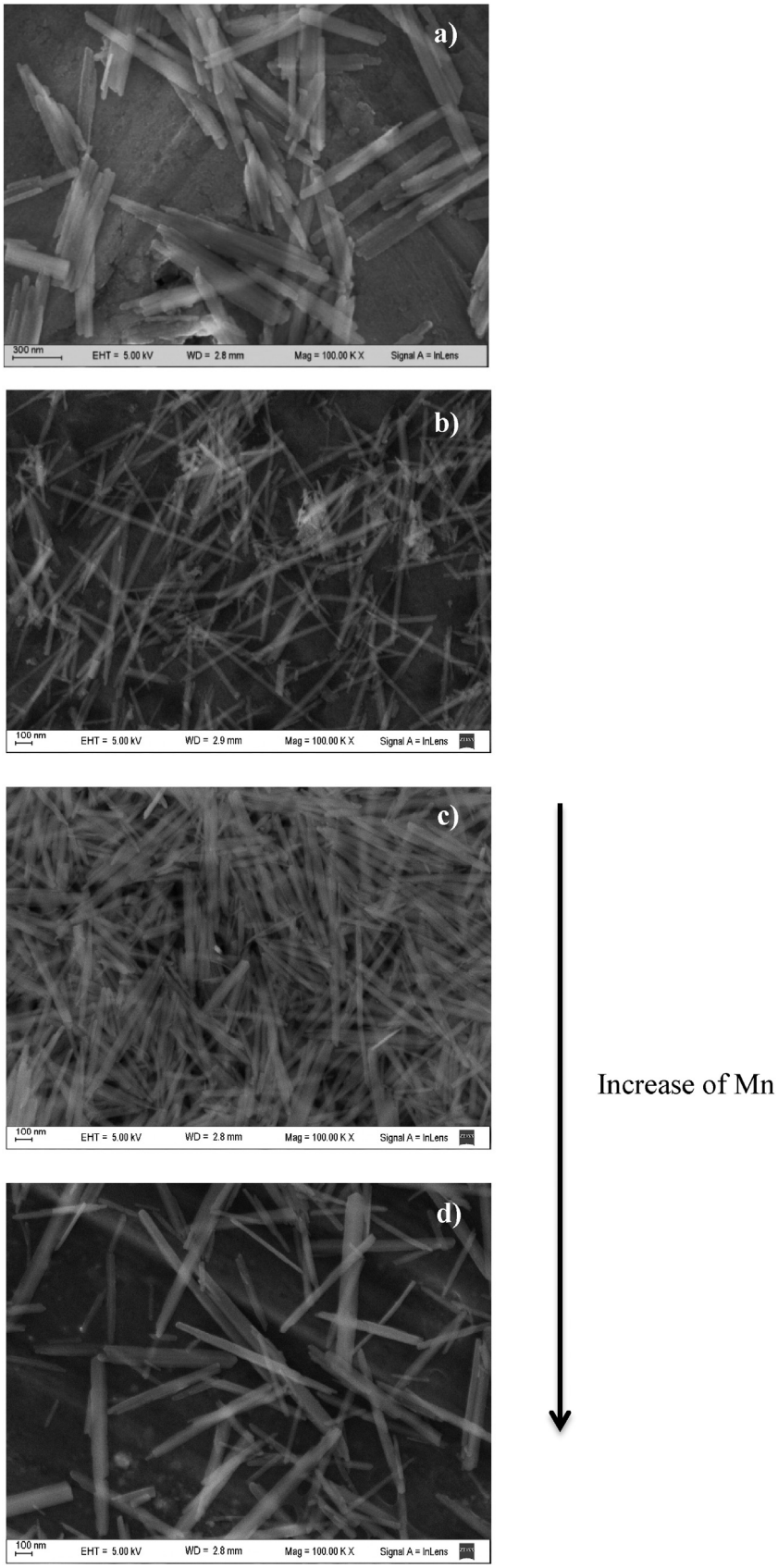

Fig. 3. Variation in the crystal morphology of goethites with an increase of structural Mn. SEM micrographs at 100,000× for samples: (a) $Co_0Mn_0Al_0$, (b) S_I–$Co_{12}Mn_0$, (c) S_I–Co_6Mn_6, (d) S_I–Co_0Mn_{12}.

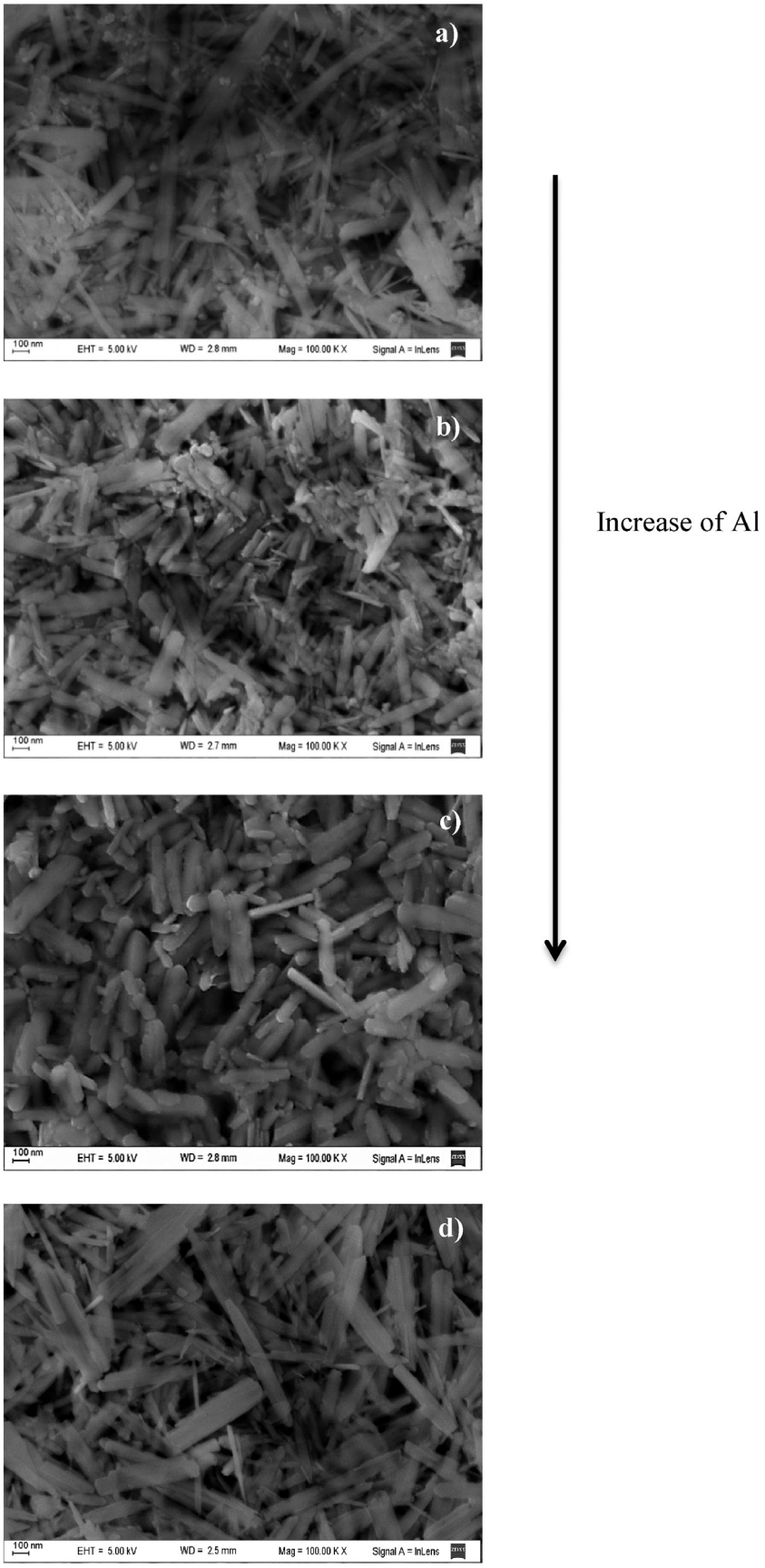

Fig. 4. Variation in the crystal morphology of Co-goethite with an increase of Al. Morphology of the tri-substituted sample. Micrographs at 100,000× for: (a) S_{II}–Co_9Al_3, (b) S_{II}–Co_3Al_9, (c) S_{II}–Co_0Al_{12}, and (d) $Co_4Al_4Mn_4$.

the surface area. The SSA followed the sequence: S_{II}–Co_6Al_6 > S_{II}–Co_9Al_3 > S_{II}–Co_3Al_9 > S_{II}–Co_0Al_{12}.

In general a correlation between crystallite size and SSA values may be found, with increasing SSA values for samples with decreasing crystallite size (cf. values for samples S_I–$Co_{12}Mn_0$, S_I–Co_0Mn_{12} and S_{II}–Co_0Al_{12}). The tri-substituted oxy(hydr)oxide presented a high SSA value ($64 \pm 1\ m^2\ g^{-1}$), consistent with the strong effect of the Co substitution. Here, the Co content was lower than that of Al and Mn; however, the influence of Co in forming particles with small crystallite size determined the enlarged surface area of the sample.

In summary, the mono-substitution of Co-for-Fe generated high SSA values, but the inclusion of Al and Mn significantly decreased these figures. The tri-substituted sample exhibited a SSA value 42% greater than the respective mono-substituted samples, in spite of a higher concentration of Al and Mn. This increase in SSA is associated with the influence of the low but significant amount of Co which was incorporated into the oxide.

3.4. Crystal morphology

The incorporations (Co-for-Fe and Mn-for-Fe) affected significantly the morphology of the acicular particles (Fig. 3 and Table 3). The mono-substitution of Co-for-Fe in goethite produced thin particles with dimensions that varied from 903 and 110 nm (length and width in pure goethite) to 567 and 29 nm in Co-goethite. These needles presented the largest L/W ratio (L: length, and W: width). Incorporation of Mn caused a slight increase in width and a significant enlargement of the particles along the *c*-axis.

The variation in the crystal morphology of Co-goethites with increasing Al-content is displayed in Fig. 4. In general, the increase in Al produced heterogeneous particles with decreased length. Pure Al-goethite (S_{II}–Co_0Al_{12}) resulted in one of the shortest needles with the smallest L/W ratio.

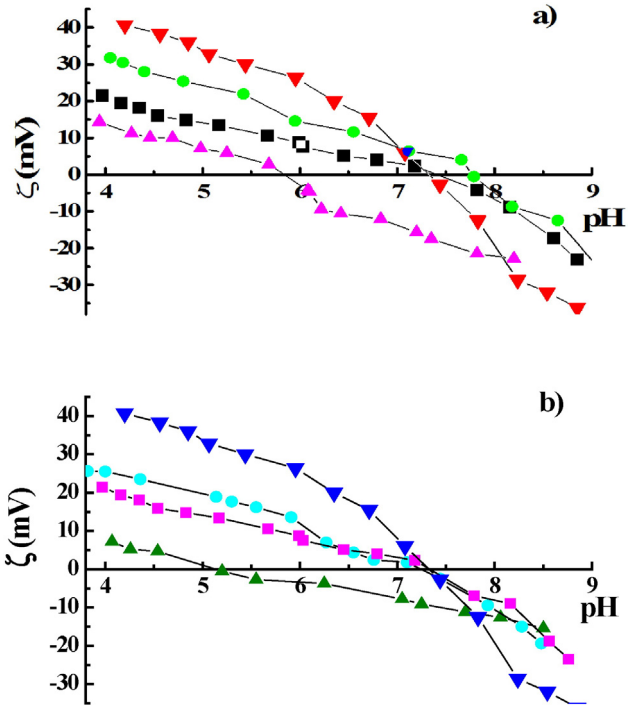

Fig. 5. Electrical charge density (ξ) *vs.* pH for selected samples in the Co-and Mn-substituted goethites, (a) (–■–) S_I–$Co_{12}Mn_0$, IEP = 7.4, (–●–)S_I–Co_6Mn_6, IEP = 7.8, (–▲–) S_I–Co_0Mn_{12}, IEP = 5.8, and (–▼–) pure goethite, IEP = 7.3; and in the Co- and Al-substituted samples (b) (–▲–) S_{II}–Co_0Al_{12}, IEP = 5.2, (–●–) S_{II}–Co_6Al_6, IEP = 7.3, (–■–) S_I–$Co_{12}Mn_0$, IEP = 7.4, and (–▼–) pure goethite.

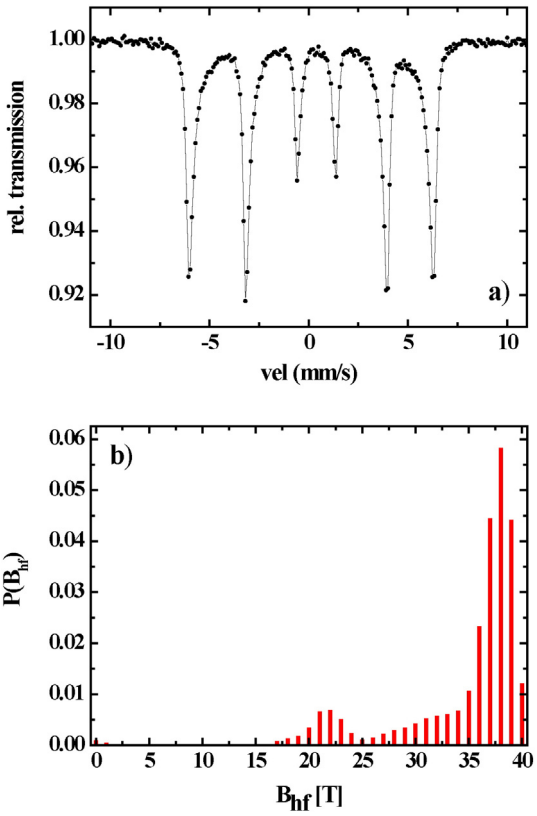

Fig. 6. RT Mössbauer spectrum (a) and its corresponding B_{hf} distribution (b) of $Co_0Al_0Mn_0$ (pure goethite).

Sample $Co_4Al_4Mn_4$ displayed varied size particles (Fig. 4 d, average width and length: 80–643 nm). These width values were close to those obtained in samples with Al-for-Fe substitution. On the other hand, the considerable length (643 nm) could be ascribed to the presence of Mn that causes highly elongated particles along the c-axis. The L/W ratio value (8.0) was intermediate between values obtained for S_{II}–Co_0Al_{12} (4.2) and S_I–Co_0Mn_{12} (14.5).

3.5. Electrophoretic mobility

Electrophoretic mobility measurements are related to the movement of suspended particles under the influence of an electric field, where the direction of the movement depends on the particles' charge at a given pH. The pH of the solution strongly influences the charge of the particles, and the pH value at which the oxide particles do not

Table 4
Mössbauer parameters for the hyperfine field distributions employed to fit the spectra.

Sample	$<B_{hf}>$ [T]	B_{hfp} [T]	IS [mm/s]	2εQ [mm/s]
$Co_0Al_0Mn_0$ (pure goethite)	35.0	38	0.41	−0.27
S_I–$Co_{12}Mn_0$	21.5	27	0.36	−0.29
S_I–Co_9Mn_3	27.0	33	0.40	−0.30
S_I–Co_6Mn_6	26.3	32	0.38	−0.28
S_I–Co_3Mn_9	25.0	30	0.38	−0.28
S_I–Co_0Mn_{12}	24.2	29	0.38	−0.28
S_{II}–Co_9Al_3	26.6	35	0.39	−0.29
S_{II}–Co_6Al_6	24.3	34	0.37	−0.31
S_{II}–Co_3Al_9	23.3	32	0.37	−0.31
S_{II}–Co_0Al_{12}	19.2	28 & 3[a]	0.36	−0.31
$Co_4Al_4Mn_4$	25.3	35	0.34	−0.32

[a] Two values with almost the same probability are found.

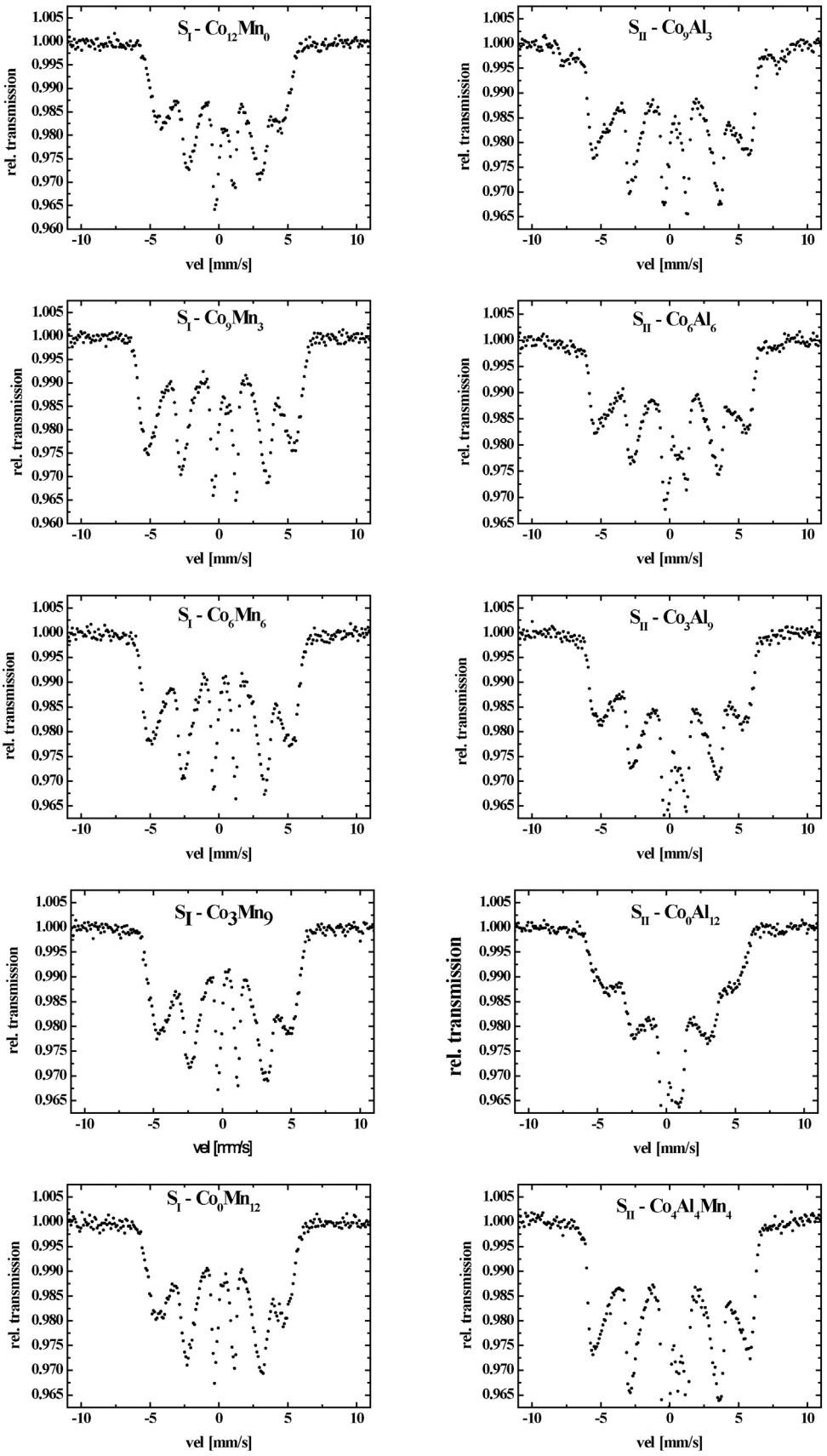

Fig. 7. Mössbauer spectra for Co-goethite samples showing the noticeable broadening of the spectral lines and a deviation from the ideal intensity ratio.

move under the applied electric field is called the point of zero charge (PZC). When electrophoretic techniques are used, the pH at which the electrophoretic mobility is zero is called the isoelectric point (IEP) (Van Olphen, 1977), and if there is no adsorption of ions other than the potential determining H^+/OH^-ions at the surface, PZC and IEP are synonymous.

The overall surface charge of goethite may be affected by the presence of foreign metal ions, and when a partial replacement of Fe(III) by other elements occurs, a shift in the value of the IEP with respect to pure goethite can be expected (Vega et al., 2004). In this work, most of the values in both series were similar to that measured for α-FeOOH (IEP = 7.3), but two samples, S_I–Co_0Mn_{12} and S_{II}–Co_0Al_{12}, displayed clearly diminished isoelectric points (Fig. 5). In the case of S_I–Co_0Mn_{12} (Mn-goethite, IEP = 5.8) the value was similar to those reported for Mn(III) oxides (<5) (Kosmulski, 2009). This indicated that the surface of the particles resembled those of Mn-oxides and that the distribution of Mn in the particles was probably concentrated toward the outer layers of the particles. Sample S_{II}–Co_0Al_{12} (Al-goethite, IEP = 5.2) displayed the smallest IEP value, and the overall most negative surface in the series; this feature can be related to the different basicity properties of the surface Fe–OH and Al–OH groups (Aquino et al., 2007). Regarding sample S_I–$Co_{12}Mn_0$ (Co-goethite, IEP = 7.4), the measured value was in agreement with data reported for cobalt oxides (Kosmulski, 2009) that show IEP values similar to that expected for pure goethite and various iron oxides (≥7). However, in this case, an inhomogeneous distribution of Co(III) in the crystals with an enrichment on the surface of the platelets cannot be discounted. Regarding the bi-substituted samples with Co + Mn or Al + Co into the structure of the oxy-hydroxide particles, the constant and almost unaltered IEP values may be caused by the simultaneous presence of two ions with opposite effects on the surface change.

3.6. Mössbauer spectroscopy analysis

The RT Mössbauer spectrum of $Co_0Al_0Mn_0$, which represents the reference goethite spectrum for the two metal substitution series exhibits asymmetrical line shapes (Fig. 6a). The data were fitted with a hyperfine magnetic field (B_{hf}) distribution (Fig. 6b), where B_{hf} is a result of the dipole interaction between the nuclear spin moment and any surrounding magnetic field. For each B_{hf} distribution two characteristic values were obtained (see Table 4): the most probable magnetic hyperfine field (B_{hfp}) and the average value ($<B_{hf}>$). In the case of sample $Co_0Al_0Mn_0$ (non-substituted, control sample), the B_{hfp} value coincided with that reported for stoichiometric, perfectly crystallized α-FeOOH (38.2 T) (Cornell and Schwertmann, 2000), but $<B_{hf}>$ was somewhat smaller (~35 T), reflecting a non-uniform particle size distribution.

The RT Mössbauer spectra of all samples in $Series_I$ and $Series_{II}$ revealed visible differences compared to the reference goethite sample, with a broadening of the spectral lines and a deviation from the ideal intensity ratio 3:2:1:1:2:3 (Fig. 7). The observed changes indicated a marked effect on the hyperfine properties of goethite when it is synthesized in the presence of Co-, Mn- and Al- ions.

Spectra for both series were also fitted with a distribution of magnetic hyperfine fields (Fig. 8).

The isomer shift, IS (which is related to the oxidation state and the chemical environment of the iron atom), and the quadrupole shift, 2εQ (which reflects the quadrupole interactions determined by the electric field gradient at the nucleus) were typical of high spin Fe(III) and remained almost constant along the series suggesting that the *s*-electron density and the symmetry of the charge distribution around the Fe nucleus were not critically affected by the substitution (Table 4).

It has been reported that the spectrum of goethite is highly influenced by the average particle size and the crystallite dimensions (Murad, 1982; De Grave et al., 2002). For example, it has been shown that the B_{hf} distribution of poorly crystallized goethite presents significant contributions at lower fields. In addition, the spectrum is also

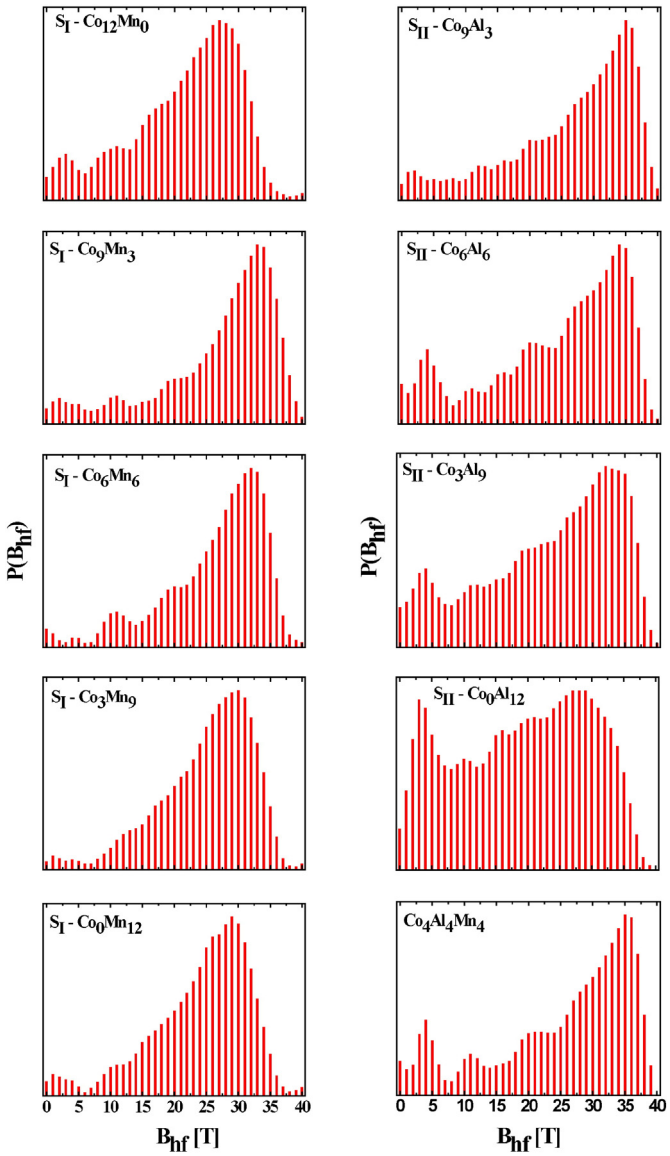

Fig. 8. Hyperfine magnetic field distributions for samples in Series I and II.

very sensitive to the incorporation of metal cations into the crystal structure, and previous studies of Co-goethites (Krehula and Musić, 2008) have demonstrated that in a series of Co-substituted goethites with similar particle and crystal sizes, the decrease of $<B_{hf}>$ could provide a measure of Co-substitution.

All $<B_{hf}>$ were lower than pure goethite including the ones corresponding to samples with enlarged crystallite size or coherent path dimensions (see for instance the L_{paral}, L_{perp} and $<B_{hf}>$ values for samples S_I–Co_0Mn_{12} and S_{II}–Co_3Al_9 in Tables 2 and 4). These results indicated that the decreased $<B_{hf}>$ values may only be attributed to Co, Mn or Al substitution into the goethite structure and/or as a consequence of a non-uniform distribution in particle size.

For both series the maxima of the B_{hf} distribution (cf. Fig. 8) were shifted toward lower B_{hf} values with decreasing Co-incorporation and, with the exception of the end members of the series Co-goethite and Mn-goethite, a quasi-linear dependence between $<B_{hf}>$ and $\chi'_{Co\text{-}goe}$ was clear in $Series_I$ (Co + Mn) (Fig. 9), indicating increasing $<B_{hf}>$ with increasing Co-incorporation.

he case of sample S_I–$Co_{12}Mn_0$ ($\chi_{Co\text{-}goe}$ = 7.4) Krehula and Musić (2008) have reported a hyperfine field value of 29 T for a Co-goethite with an approximate cobalt content ($\chi_{Co\text{-}goe}$ = 6.98). The value obtained in this work (21.5 T) is markedly lower and could be ascribed to the

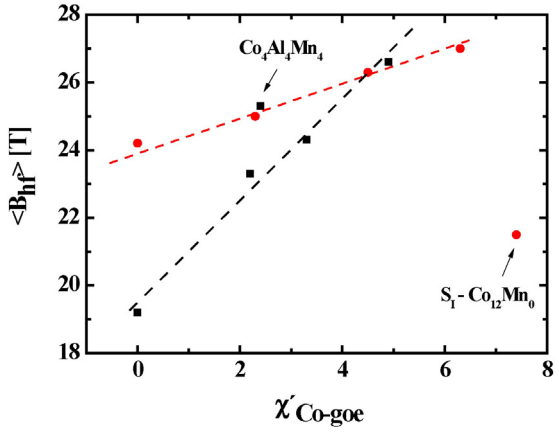

Fig. 9. <B_{hf}> *vs.* Co-content in the formed goethites for Series$_I$ (●) and Series$_{II}$ (■) samples. Dotted lines are only a guide to the eye.

small particle size of the sample that results in a high specific surface area (109.45 ± 1 $m^2\ g^{-1}$). The presence of these small particles was reflected in the hyperfine field distribution graphic (Fig. 8) that showed superparamagnetic contributions at B_{hf} values less than 7 T.

Regarding sample S_I–Co_0Mn_{12} ($\chi_{Mn\text{-}goe.} = 10.2$), we have found a < B_{hf} > value of 24.2 T that was also lower than the reported values (29.4 and 26.9 T) for two samples of Mn-goethites ($\chi_{Mn\text{-}goe} = 9.09$ and 11.1, Krehula and Musić, 2006). The decreased value may be attributed to differences in particle and crystallite sizes derived from a completely different sample preparation.

In Series$_{II}$ (Co + Al) instead, the effect of the Al incorporation led to a spectrum with a similar appearance to the ones produced by small particles (Ferreira et al., 2003). Furthermore, an increase in the Al content caused a decrease in <B_{hf}> values that was more pronounced than in the case of Series$_I$ with Mn-incorporation (see Fig. 7).

The distributions shown in Fig. 8 revealed a significant superparamagnetic contribution at B_{hf} < 7 T in the Al-containing samples that was mainly caused by the diamagnetic character of the Al(III) cations, the presence of which produced an interruption in the superexchange between the Fe–O–Fe chains – which control the magnetic order – in the goethite structure. The distribution of particle size also contributed to this behavior. It is interesting to note that in S_{II}–Co_0Al_{12} there were two B_{hfp} values with almost the same probability in the hyperfine field distribution (Fig. 8 and Table 4). The lower value, ca. 3 T, was consistent with the shortest needles and the smallest L/W ratio displayed in Table 3 for this sample.

The linear tendency in these samples was not as accurate as in Series$_I$ because of the contribution of the Co-ferrite fraction to the spectra in S_{II}–Co_9Al_3 and S_{II}–Co_6Al_6 (see for example the enlarged spectrum of S_{II}–Co_9Al_3 in Fig. 10).

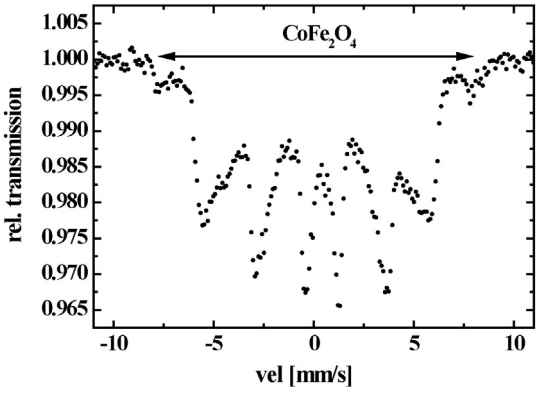

Fig. 10. Cobalt ferrite contribution in S_{II}–Co_9Al_3 sample Mössbauer spectrum.

Literature data indicate that the cobalt ferrite Mössbauer spectrum is usually fitted by the superposition of several sextets (Ferreira et al., 2003). However in the present work, as it represents a minor contribution, for the sake of simplicity it was fitted with only one broad sextet with a hyperfine field near 47 T, confirming that the spinel phase determined by XRD analysis corresponds to Co-ferrite.

The dissimilar B_{hf} value encountered for the tri-substituted sample, $Co_4Al_4Mn_4$ (see Fig. 9) may be attributed to the concomitant action of Mn and Al, without discarding particle size effects.

4. Conclusions

The transformation of ferrihydrite to goethite in a basic medium, and in the simultaneous presence of cations that are associated with iron oxides in soils and sediments (Co(II) + Mn(II), Co(II) + Al(III), Co(II) + Mn(II) + Al(III)) produced bi- and tri-substituted goethites with variable structural, surface and hyperfine properties. No synergetic or antagonistic effects have been detected, and prior to incorporation, and the manganese and cobalt ions were oxidized to their Me(III) form.

The specific surface areas and the particle sizes were greatly influenced by the foreign cations incorporation, and an increase in Co-content determined increased SSA values and decreased particle sizes. As these changes are closely related to the chemical reactivity of the substituted goethites, enhancing or retarding its dissolution behavior, the reported results lead to a better understanding of the fate and transport of these cations near a water-solid interface. The reported SSA is also a relevant data that will contribute to elucidate the role played by multi-substituted goethites in remediation processes where a large SSA value is desirable for a greater adsorption capacity of contaminants. In contrast, the bi-substitution did not alter noticeably the IEP values of pure goethite, suggesting that the incorporation of Co + Mn or Co + Al did not play an important role in changing the surface charge characteristics, and consequently the adsorption properties of the solid.

The Mössbauer spectra of the multi-substituted samples, showing a broadening of the spectral lines and a deviation from the ideal intensity ratio 3:2:1:1:2:3, and the lowering in <B_{hf}> when the Co-content in the goethite is decreased, are hyperfine properties that may help in the analyses of natural substituted samples.

Acknowledgments

This research was supported by grants PICT 2008-0780 (Agencia Nacional de Promoción Científica y Tecnológica) and 24/Q051 (Secretaría de Ciencia y Tecnología, UNS). Authors are also thankful to Consejo Nacional de Investigaciones Científicas y Técnicas de la República Argentina (CONICET).

References

Alvarez, M., Sileo, E.E., Rueda, E.H., 2005. Effect of Mn(II) incorporation on the transformation of ferrihydrite to goethite. Chem. Geol. 216, 89–97.
Alvarez, M., Rueda, E.H., Sileo, E.E., 2007. Simultaneous incorporation of Mn and Al in the goethite structure. Geochim. Cosmochim. Acta 71 (4), 1009–1020.
Alvarez, M., Sileo, E.E., Rueda, E.H., 2008. Structure and reactivity of synthetic Co-substituted goethites. Am. Mineral. 93, 584–590.
Aquino, A.J., Tunega, D., Haberhauer, G., Gerzabek, M.H., Lischka, H., 2007. Quantum chemical adsorption studies on the (110) surface of the mineral goethite. J. Phys. Chem. C 111 (2), 877.
Brand, R.A., 1991. Normos Programs (SITE-DIST). Duisburg University.
Cornell, R.M., 1991. Simultaneous incorporation of Mn, Ni and Co in the goethite (α-FeOOH) structure. Clay Miner. 26, 427–430.
Cornell, R.M., Schwertmann, U., 2000. The Iron Oxides, Structure, Reactions, Occurrence and Uses. 2nd ed. VCH, Weinheim, Germany.
De Grave, E., Barrero, C.A., Da Costa, G.M., Vandenberghe, R.E., Van San, E., 2002. Mössbauer spectra of α-and γ-polymorphs of FeOOH and Fe_2O_3: effects of poor crystallinity and of Al-for-Fe substitution. Clay Miner. 37, 591–606.
Dos Santos, A.C., Horbe, A.M.C., Barcellos, C.M.O., Marimon da Cunha, J.B., 2001. Some structure and magnetic effects of Ga incorporation on α-FeOOH. Solid State Commun. 118, 449–452.

Ferreira, T.A.S., Waerenborgh, J.C., Mendonça, M.H.R.M., Nunes, M.R., Costa, F.M., 2003. Structural and morphological characterization of $FeCo_2O_4$ and $CoFe_2O_4$ spinels prepared by a coprecipitation method. Solid State Sci. 5, 383–392.
González, E., Ballesteros, M.C., Rueda, E.H., 2002. Reductive dissolution kinetics of Al-substituted goethites. Clays Clay Miner. 50 (4), 470–477.
Guimaraes, I.R., Giroto, A., Oliveira, L.C.A., Guerreiro, M.C., Lima, D.Q., Fabris, J.D., 2009. Synthesis and thermal treatment of Cu-doped goethite: oxidation of quinoline through heterogeneous Fenton process. Appl. Catal. B Environ. 91, 581–586.
Kaur, N., Gräfe, M., Singh, B., Kennedy, B.J., 2009a. Simultaneous incorporation of Cr, Zn, Cd, and Pb in the goethite structure. Clays Clay Miner. 57 (2), 234–250.
Kaur, N., Singh, B., Kennedy, B.J., 2009b. Copper substitution alone and in the presence of chromium, zinc, cadmium and lead in goethite (α-FeOOH). Clay Miner. 44 (3), 293–310.
Kosmulski, M., 2009. Compilation of PZC and IEP of sparingly soluble metal oxides and hydroxides from literature. Adv. Colloid Interface Sci. 152, 14–25.
Krehula, S., Musić, S., 2006. Influence of Mn-dopant on the properties of α-FeOOH particles precipitated in highly alkaline media. J. Alloys Compd. 426, 327–334.
Krehula, S., Musić, S., 2008. Influence of cobalt ions on the precipitation of goethite in highly alkaline media. Clay Miner. 43 (1), 95–105.
Krehula, S., Musić, S., 2009. The influence of a Cr-dopant on the properties of α-FeOOH particles precipitated in highly alkaline media. J. Alloys Compd. 469, 336–342.
Krehula, S., Musić, S., Popović, S., 2005. Influence of Ni-dopant on the properties of synthetic goethite. J. Alloys Compd. 403, 368–375.
Larson, A.C., Von Dreele, R.B., 1996. General structure analysis system (GSAS). Los Alamos National Laboratory Report LAURpp. 86–748.
Long, G.J., Cranshaw, T.E., Longworth, G., 1983. The ideal Mössbauer effect absorber thickness. Mössbauer Effect Ref. Data J. 6, 42–49.
Manceau, A., Schlegel, M.L., Musso, M., Sole, V.A., Gauthier, C., Petit, P.E., Trolard, F., 2000. Crystal chemistry of trace elements in natural and synthetic goethite. Geochim. Cosmochim. Acta 64, 3643–3661.
Murad, E., 1982. The characterization of goethite by Mössbauer spectroscopy. Am. Mineral. 67, 1007–1011.
Murad, E., Bowen, L.H., 1987. Magnetic ordering in Al-rich goethites; influence of crystallinity. Am. Mineral. 72, 194–200.
Murad, E., Johnston, J.H., 1987. Mössbauer Spectroscopy Applied to Inorganic Chemistry. Plenum Publishing Corporation, New York, pp. 507–582.
Schwertmann, U., Taylor, R.M., 1989. In: Dixon, J.B., Weed, S.B. (Eds.), Minerals in Soil Environments. Soil Sci. Soc. Am, Madison, WI, pp. 380–438.
Shannon, R.D., 1976. Revised effective ionic radii and systematic studies of interatomic distances in halides and chalcogenides. Acta Crystallogr. Sect. A: Found. Crystallogr. 32, 751–767.
Sileo, E.E., Alvarez, M., Rueda, E.H., 2001. Structural studies on the manganese for iron substitution in the synthetic goethite–jacobsite system. Int. J. Inorg. Mater. 3, 271–279.
Sileo, E.E., García, Rodenas L., Paiva-Santos, C.O., Stephens, P.W., Morando, P.J., Blesa, M.A., 2006. Correlation of reactivity with structural factors in a series of Fe(II) substituted cobalt ferrites. J. Solid State Chem. 179 (7), 2237–2244.
Singh, B., Gräfe, M., Kaur, N., Liese, A., 2010. Applications of synchrotron-based x-ray diffraction and x-ray absorption spectroscopy to the understanding of poorly crystalline and metal-substituted iron oxides. Dev. Soil. Sci. 34, 199–254.
Szytula, A., Burewicz, A., Dimitrijevic, Z., Krasnicki, S., Rzany, H., Todorovic, J., Wanic, A., Wolski, W., 1968. Neutron diffraction studies of α-FeOOH. Phys. Status Solidi B 26 (2), 429–434.
Thompson, P., Cox, D.E., Hastings, J.B., 1987. Rietveld refinement of Debye–Scherrer synchrotron X-ray data from Al_2O_3. J. Appl. Crystallogr. 20, 79–83.
Toby, B.H., 2002. EXPGUI, a graphical user interface for GSAS. J. Appl. Crystallogr. 34, 210–213.
Van Olphen, H., 1977. An Introduction to Clay Colloid Chemistry. Wiley, NewYork, NY.
Vandenberghe, R.E., 1991. Mössbauer Spectroscopy and Applications in Geology. Apostilha International Training Centre for Post-Graduate Soil Scientists.
Vega, F.A., Covelo, E.F., Andrade, M.L., Marcet, P., 2004. Relationships between heavy metals content and soil properties in mine soils. Anal. Chim. Acta 524, 141–150.